

Validation and Error Analysis of  
OSCAR Sea-surface Currents

Eric S. Johnson, Fabrice Bonjean, Gary S. E. Lagerloef, and John T. Gunn

*Earth and Space Research, Seattle WA, USA*

Gary T. Mitchum

*College of Marine Science, University of South Florida, St. Petersburg FL, USA*

corresponding author:

Eric S. Johnson,  
1910 Fairview Ave. E. Suite 210  
Seattle, Washington 98102 U.S.A.  
ejohnson@esr.org, 206-440-1863

Revised for Journal of Atmospheric and Oceanic Technology, 21 April 2006

## ABSTRACT

Comparisons of OSCAR satellite-derived sea surface currents with *in situ* data from moored current meters, drifters, and shipboard current profilers indicate that OSCAR presently provides accurate time-means of zonal and meridional currents, and in the near-equatorial region reasonably accurate time variability (correlation = 0.5 to 0.8) of zonal currents at periods as short as 40 days and meridional wavelengths as short as  $8^\circ$ . At latitudes higher than  $10^\circ$  the zonal current correlation remains respectable but OSCAR amplitudes diminish unrealistically. Variability of meridional currents is poorly reproduced, with severely diminished amplitudes and reduced correlations relative to those for zonal velocity on the equator. OSCAR's RMS differences from drifter velocities are very similar to those experienced by the ECCO data-assimilating models, but OSCAR generally provides a larger ocean-correlated signal which enhances its ratio of estimated signal over noise. Several opportunities exist for modest improvements in OSCAR fidelity even with presently available data sets.

### 1. Introduction

The unique power of satellite-derived products is their comprehensive global coverage in both space and time. Yet this same breadth of coverage makes validation very difficult, since no ground-based data set offers sufficient coverage to allow exhaustive comparison. Here we validate the OSCAR sea surface currents (SSC), a product constructed from TOPEX/Poseidon sea surface heights (SSH), scatterometer winds (W), and both AVHRR and *in situ* sea surface temperatures (SST) (Bonjean and Lagerloef 2002). Previous investigators have estimated the errors of satellite-derived SSH and SSC, essentially by propagating the satellite data's expected measurement errors through the calculations and interpolations required to extend raw data along the satellite ground tracks to a comprehensive product. This requires detailed knowledge of the

space and time scales of the process being estimated (e.g. SSC), which generally was constructed from reasonable assumptions (Le Traon and Dibarboure 1999, Ducet et al. 2000, Schlax and Chelton 2003) or through use of general circulation model output (Leeuwenburgh and Stammer 2002). A more stringent test, however, is to compare the satellite product to actual ground truth. Thus we assemble here a relatively exhaustive collection of available ground-based velocity data to test the OSCAR product's ability to reproduce the temporal and spatial variability of real ocean currents.

### *Analysis approach*

Throughout the analysis our approach will be to subsample and interpolate the OSCAR currents to the times and locations of the comparison data. This ensures our results will reflect the various data sets' ability to measure jointly sampled ocean variability, with any discrepancies being due to measurement error rather than to disparate coverage in space and time. Of course this also means that we can validate the OSCAR product only when and where independent measures of ocean currents exist. In particular we focus on the tropical Pacific Ocean as the region currently covered by OSCAR. To the extent that other regions have differing ocean phenomena the present results may be less applicable there.

## **2. OSCAR Methodology**

### *a. Data sources*

OSCAR currents are calculated at 5-day intervals, with each 5-day map being derived from previously gridded maps of SSH, W, and SST representing the surrounding ~10 days of data. The source datasets are built mainly from satellite data that have been collected since

October 1992 during on-going missions. SSH is gridded from TOPEX/POSEIDON data for the period Oct. 1992 to June 2002, and from JASON-1 for the period from July 2002 to present (Lagerloef et al. 1999).  $W$  is provided by the variational analysis Special Sensor Microwave Imager (SSM/I) winds (Atlas et al. 1996; October 1991 to September 2001) and the QuickScat gridded winds from COAPS (August 2001 to present). For SST we use Reynolds and Smith's version 2 SST, a product blended from satellite and *in situ* data (Reynolds et al. 2002). The OSCAR dataset is routinely updated every week, and covers the period from Oct. 1992 to within about 8 to 14 days of the present.

### *b. Momentum balance*

The OSCAR method for calculating ocean near-surface velocity is based on the resolution of quasi-linear and quasi-steady momentum equations (Bonjean and Lagerloef 2002). Since local acceleration is neglected this diagnostic calculation requires no time-integration, but is also only valid for low-frequency motions. The final velocity field is a combination of geostrophic, Ekman/Stommel, and thermal-wind currents. These approximations are singular near the equator where the Coriolis parameter  $f$  tends toward zero. The OSCAR method surmounts this singularity as follows. For the combined geostrophic, Ekman/Stommel, and thermal-wind approximations to be rigorously valid near the equator the dominant non-geostrophic momentum terms, that is the pressure gradient force and drag force from the wind, must balance to zero-order. In the OSCAR diagnostic model this requirement is met by fixing one of the two free parameters, the depth-scale  $H$ , to a value of 70 m based on a fit to extensive observations.

With the dominant non-geostrophic balance satisfied (and neglecting other terms) equatorial velocity becomes the sum of geostrophic, Stommel and thermal-wind terms, providing

each are expanded as a Taylor series to first order around the latitude  $y=0$  (hence equatorial geostrophic velocity is proportional to the second derivative of the SSH as used by numerous previous studies). Since this balance is derived from simplified physics it is not expected to hold exactly at all times and longitudes; but any residual would imply infinite geostrophic velocities at the equator and so must be removed. For this, a weak formulation of the momentum equations is solved using a basis set of 12 orthogonal polynomials to approximate the velocity solution as a function of latitude between  $8^\circ\text{N}$  and  $8^\circ\text{S}$ . This results in continuous profiles across the equator. Poleward of  $8^\circ$  the classical formulations of geostrophic, wind-driven and thermal-wind terms are used and joined with the equatorial solution using a linear taper-function between  $5^\circ$  and  $8^\circ$  latitude.

The second free parameter in the diagnostic model is the coefficient of turbulent vertical momentum diffusion,  $A$ , which is parameterized as an approximately linear function of the wind speed squared consistent with past studies (Santiago-Mandujano and Firing 1990). In effect the inverse of this parameter scales the magnitude of the wind-forced Ekman/Stommel flow. OSCAR currents are designed to represent the average over a surface layer 30 m thick.

Note that the current OSCAR diagnostic model is not adjusted to fit *in situ* measurements, in particular the 15m-drogued drifter data, as was the case in the previous analysis of Lagerloef et al. (1999).

### *c. Mean Dynamic Topography*

Since the absolute geoid height is not accurately inferred from altimetric satellites (TOPEX/POSEIDON, JASON-1) only the time-varying portion of altimetric SSH is used to compute geostrophic velocity. The absolute geostrophic velocity is added by replacing the

altimetric SSH mean with a separately determined mean dynamic topography field (MDT). This MDT is derived from multiple data sets, including *in situ* and satellite data, by Rio and Hernandez (2004). Since the *in situ* data includes drifting buoy data from the period 1993-1999 the time-mean OSCAR currents are not entirely independent of this data in the validations presented here.

### **3. Reference Data**

#### *a. Surface Drifters*

Our primary ground-based data set, both in quantity and coverage, is the Global Lagrangian Drifting Buoy data base compiled and made available by the Atlantic Oceanographic and Meteorological Laboratory (Pazan and Niiler 2004). The buoys' drogue depth of 15 m is reasonably representative of the 0-30 m surface layer measured by OSCAR. Thus we use only buoys with intact drogues, block-averaged to daily intervals. Individual buoys sample closely in time but are sparsely scattered in space. Therefore we will treat this data set primarily as a collection of time series taken at scattered locations throughout the ocean. Since the buoys drift relatively slowly we anticipate that most of their measured variability will be temporal rather than spatial.

#### *b. Moored Current Meters (MCMs)*

Daily-averaged MCM data are provided by the Pacific Marine Environmental Laboratory from equatorial moorings at 110, 140, and 170°W and 165°E. We use primarily the moored ADCP data but insert mechanical current meter data where ADCP data are not available, particularly the missing 10 m data; thus "MCM" refers here to a "Moored" current meter rather

than exclusively a “Mechanical” one. Occasional data gaps at individual instrument depths were filled from the two nearest depths using a least-mean-square error estimator constructed from correlations between existing data at those depths, then adjusted in amplitude to match the target depth’s historical variance. Only estimators demonstrating a historical correlation to the target data of 0.85 or better were used. These estimated time series were substituted directly into data gaps in the case of meridional velocity, where the long-term mean is small and high-frequency variability is large. For zonal velocity, however, estimated time series were faired into the data gap by adding a linear time trend so that the resulting estimate matched the three days of observations on either side. This adjusts the estimated zonal currents to better match the time-local vertical shear, which can change substantially. The current time series were then extrapolated from 10 m depth to the surface using constant shear, and the average over the 0-30 m surface layer constructed using trapezoidal integration.

### *c. Acoustic Doppler Current Profilers (ADCP)*

The shipboard ADCP data used here are selected from roughly meridional sections spanning the tropical Pacific from 8°S to 15°N (Johnson and Proehl 2004). Data were extracted from cruises of the US Joint Global Ocean Flux Study (JGOFS) Equatorial Pacific Process Study (Murray et al. 1995), the World Ocean Circulation Experiment (WOCE, Firing et al. 1998), the Tropical Ocean-Atmosphere (TAO) mooring maintenance cruises (years 1991-1995 from E. Johnson and Plimpton 1999, years 1996-2001 provided by Eric Firing), and the Tropical Ocean Climate Study (TOCS, Kashino et al., 2001). The JGOFS data and early TAO data were processed by E. Johnson and Plimpton (1999); the remaining data were acquired from the NODC shipboard ADCP archive and were processed by various investigators as referenced in the individual data meta files. Here we have spatially gridded the 1-5 minute time-averaged data

into  $0.1^\circ$  latitude bins, substantially reducing instrument noise while retaining full meridional resolution of the large-scale current variability. We use the shallowest depth measured, generally around 20 m, as representative of the surface layer. The sections are scattered across the Pacific ocean with generally no more than 2 or three sections per year available at a given longitude. Johnson and Proehl (2004) found these data were too few to distinguish even large-scale, long-term ocean variability from higher-frequency noise; thus we use the ADCP sections here as snapshots in time of the ocean's meridional structure. Occasional gaps of up to  $1.5^\circ$  latitude in individual sections were filled using a combination of beam and Laplace's equations to give smooth interpolations without overshoot (Johnson and Proehl 2004).

#### *d. ECCO Model Simulations*

We use ECCO (Consortium for Estimating the Circulation and Climate of the Ocean) model output as examples of velocity products produced by modern general circulation models with advanced data assimilation schemes, an alternative to the simplified physics of the OSCAR velocity algorithm. We compare ECCO 15 m velocities to surface drifters exactly as with the OSCAR velocities. The ECCO-1 model produced at Scripps Institution of Oceanography outputs monthly fields on a  $1 \times 1$  degree grid. This model was forced by NCEP surface fluxes; it also used an adjoint method to assimilate monthly climatologies of temperature, available *in situ* measurements of temperature and salinities, SSH from ERS and TOPEX/Poseidon, and the mean velocity of accumulated surface drifters (Stammer et al. 2002). The ECCO-2 simulation produced by NASA's Jet Propulsion Laboratory gives 10-day fields. It also has a  $1 \times 1$  degree grid except that meridional resolution gradually improves to 0.3 degrees within 10 degrees of the equator. It is forced by NCEP winds and surface fluxes with means replaced by those of COADS, and uses a Kalman filter to assimilate the time variability of TOPEX/Poseidon SSH

(Fukumori 2002). Surface SST and SSS are further relaxed to observed values.

## 4. Results

### *a. Mean comparison of OSCAR with drifters, ADCP, and ECCO*

As mentioned above we sub-sample and interpolate the gridded OSCAR currents in space and time to match each validation data set, and gather statistics from these mutually defined data. This eliminates disparities in coverage, ensuring that any discrepancies between the paired data are directly interpretable as instrumental noise or other shortcomings rather than differently sampled ocean variability. The time-averaged OSCAR currents compare well to both the drifter and ADCP currents (Fig. 1). Due to differing time and space coverage there will be slight differences between the means of the ADCP and drifter currents, and those differences will be reflected in the matched OSCAR currents as well. The time means of drifter and matched OSCAR currents agree very closely at all latitudes in both longitude ranges. The only systematic difference is a tendency of OSCAR to overestimate meridional velocity. The comparison between OSCAR and ADCP currents shows larger though still modest discrepancies. OSCAR consistently underestimates the strengths of ADCP zonal currents, and at 200-150°W overestimates ADCP meridional currents even more than for drifter currents. At 150-100°W the ADCP meridional flow is clearly asymmetric about the equator, a feature entirely missed by OSCAR. It is useful to recall that drifter measurements were incorporated into the OSCAR mean dynamic topography (Rio and Hernandez 2004), so that only the ADCP data offer a completely independent measure of mean ocean currents. Also, the mean zonal currents shown here have a small sampling bias of about +15 cm/s at the equator in the western Pacific, indicated by the fact that both the drifters and the matching OSCAR currents have time means differing by that amount from the comprehensive time mean of OSCAR over the available

period.

The two ECCO model simulations produce mean currents that are less realistic (Fig. 2). The simulations' mean zonal currents are somewhat attenuated relative to the drifters', and while meridional currents are better the ECCO1 equatorial divergence tends to be weak. These model simulations cover slightly different periods than the OSCAR data (a difference of some 400 days out of 12 years of data) but this does not introduce significant bias in that the drifter means from each of the three comparisons agree to within a few cm/s.

*b. OSCAR/MCM Time domain variability*

MCM data provide the most straightforward look at OSCAR's ability to replicate ocean variability, since they are traditional time series of Eulerian currents at fixed locations. Their equatorial location provides an especially interesting test since OSCAR currents are essentially a geostrophic calculation. Direct comparison between MCM currents and interpolated OSCAR currents shows that the lower-period variability of zonal currents is well reproduced; but the higher-frequency, tropical instability wave (TIW) variability that dominates meridional velocity is measured poorly if at all (Fig. 3). Coherence calculations confirm that zonal currents are measured with good fidelity at periods longer than 40 days, but meridional currents are not well measured at any period (Fig. 4). Meridional velocity at 110°W is significantly coherent around 30-90 days period, but the OSCAR amplitudes are much too low (not shown) making the actual fidelity poor. Dividing the OSCAR product into Ekman (wind-forced) and Geostrophic (pressure gradient- and buoyancy-forced) components reveals much the same result for the Geostrophic component (not shown), but interestingly a statistically significant phase lag for the Ekman component's shorter periods (Fig. 5). The time equivalent of the phase lags (equal to the fractional lag times period) is around 10 days over periods ranging from 20 to 90 days. This is a

reasonable response time for near-equatorial motions, and suggests that including a time derivative in the OSCAR algorithm would improve its fidelity.

*c. OSCAR/Drifter Time domain variability*

Surface drifters provide velocity information that is scattered broadly in space with little resolution. Analyzing the time variability of such data (and matched OSCAR currents) is a challenge. Individual drifter time series are relatively short (<1 year) in duration, yet during that period often travel far enough to sample distinctly different current regimes. This confusion of temporal and spatial variability is an inherent difficulty of Lagrangian measurements. We reduce the problem here by removing the true time average of OSCAR currents from both the drifter and OSCAR velocities before comparison; thus at least the relatively strong time-mean current structure will not be aliased into temporal variability. The resulting demeaned data are analyzed for frequency content. For such short time series Fourier transform techniques as used for the MCM data above are not well suited: the fundamental Fourier assumption of time-cyclical data results in the variance associated with differences between series end-points being scattered across all frequencies. Instead we low-pass filter the individual drifter time series with a hierarchy of Gaussian-shaped filters having increasingly long period filter cut-offs. We then difference the variances retained by each successive filter to estimate the variance associated with the intervening frequency bands. This approach conserves data variance by construction, whereas forming band-passed time series and then taking statistics directly would not: band-passed series are not truly independent of their residuals unless the frequency cut-offs are abrupt, which returns us again to the difficulty of using Fourier techniques. The filter cut-offs will be reported here as those periods (and later wavelengths) having half-power response; Gaussian filters pass about 2.8 independent points per half-power period, so the minimum time scale

passed is smaller than the reported cut-off period by that factor.

Having band-passed both the drifter data and the matched OSCAR currents we bin them in longitude and latitude as with the means above. In each bin we remove residual means from the drifter and OSCAR data, representing true mean differences between the two and incomplete sampling relative to the all-time OSCAR mean removed earlier. The resulting drifter RMS velocities associated with each frequency band are shown in Fig. 6. As expected zonal velocity has a red spectrum markedly peaked at the equator, where it roughly matches comparable bands extracted from the MCM analysis above (plotted as circles). Meridional velocity is also peaked at and north of the equator in the eastern Pacific, consistent with the dominating presence of TIWs, but the spectral peak at 10-20 day periods seen clearly in the MCM analysis is somewhat broadened here in the drifter analysis.

The zonal rms velocity of matched OSCAR currents shows a comparable spatial structure near the equator (Fig. 7); but meridional velocity is poorly captured as was also found in the MCM analysis. Both velocity components are increasingly underestimated as one proceeds poleward, a trend no doubt contributed to by the poleward-diminishing Rossby radius that favors features too small to be resolved by the satellite ground tracks. The variance of OSCAR velocities as matched to drifter tracks tends to be higher than the comparable variance of OSCAR velocities as matched to fixed MCM locations (circles), especially for shorter periods. We take this as confirmation that some spatial variability has been aliased by the moving drifters, and thus we regard the shorter-period results with some caution.

The band-passed correlation (equivalent to the in-phase coherence) between drifter and matched OSCAR zonal velocities is remarkably good, peaking around the North Equatorial Countercurrent (NECC) at 6-8°N and diminishing poleward (Fig. 8). Longer period motions are

measured best, but as with the MCM analysis appreciable skill extends down through 40 day periods. Interestingly the equator is a nadir for meridional velocity correlation, which then increases poleward with the best values again in the NECC region. Otherwise correlation is relatively constant across the longer period bands (>40 days). This correlation derives mostly from the geostrophic component of OSCAR currents, though at periods greater than 80 days the Ekman component contributes some (not shown).

*d. OSCAR/ADCP Space domain variability*

ADCP sections give us approximate snapshots in time of the meridional structure of ocean currents at scattered locations. Adapting the analysis used above in the OSCAR/Drifter comparison we remove the OSCAR time means from the ADCP data and interpolate OSCAR velocities to match each section, then filter the paired OSCAR/ADCP sections in latitude exactly as we filtered the drifter-derived series in time: from this we estimate the OSCAR product's fidelity to "true" ocean currents at various meridional wavelengths. Again the filter cut-offs are reported as half-power wavelengths, each comprising 2.8 independent spatial scales. Matched OSCAR currents reproduce the RMS magnitude of ADCP zonal currents well at meridional wavelengths of 16° and longer, but increasingly poorly at shorter wavelengths. RMS meridional velocity is not well reproduced at any wavelength (Fig. 9). As found for the drifters the correlation between ADCP and OSCAR zonal currents is high, though substantially diminished at wavelengths shorter than 4° latitude. For meridional velocity correlation is poor, though for longer wavelengths it improves away from the equator (not shown) much as in the drifter analysis (Fig. 8).

*e. Other surface current products*

We repeat our above comparison between surface drifters and OSCAR currents by substituting for the canonical OSCAR product a number of alternate surface current products. These include several versions of OSCAR incorporating alternate SSH fields, and the two ECCO data-assimilating GCMs previously used. Rather than report the calculations in detail we summarize by showing an approximate signal to noise ratio for each product (Fig. 10): that is, the RMS velocity of the specified current product divided by its RMS difference from matching drifter currents. The RMS difference will contain not only errors in the product's reproduction of large-scale circulation but also additional noise associated with the drifter's sampling of small, local features not included in the large-scale product. Our efforts to quantify this additional small-scale variability using spatially resolved ADCP data have proved to be too dependent upon analysis assumptions to be reliable: thus we have not removed estimated small scale variability from the RMS differences, and the RMS differences reported here must be considered upper limits on a product's error as a measure of large-scale circulation.

The alternate OSCAR current products include calculations substituting SSH fields gridded by AVISO from TOPEX/Poseidon/ Jason, ERS-1 and ERS-2 data (denoted AVISO, Ducet et. al 2000); calculations substituting AVISO SSH fields gridded from TOPEX/Poseidon-Jason alone (denoted AVISO/TPJ); and calculations substituting a gridded SSH field from the Naval Research Laboratories (denoted NRL; Greg Jacobs personal communication). Surface current calculations completely independent of OSCAR are represented by the two ECCO simulations detailed above. All five products were independently matched to available drifter tracks and low-pass filtered to 20-day period as above. The results indicate that, at least by this measure of signal/noise, the OSCAR-based calculations substantially surpass the ECCO simulations at all locations in their ability to duplicate drifter currents (but see discussion). Interestingly, everywhere but in the equatorial western Pacific the AVISO SSH fields prove

more useful than our conventional TOPEX/Poseidon-Jason analysis, while the NRL field is roughly equivalent in usefulness. The improved AVISO fidelity occurs mostly in the 20-40 day band (not shown), where AVISO-derived currents are substantially better than the current OSCAR product. Inclusion of ERS-1 and -2 data in AVISO SSH (AVISO compared to AVISO/TPJ) does not result in substantial improvement for this application (but see discussion). The fidelity of all products increases with additional filtering to lower frequencies, but their relative standing remains the same.

*f. OSCAR/drifter monthly maps*

Previous results focused on the time variability of OSCAR currents as being in effect our contribution to the estimation of surface currents, with the MDT calculated by others. Yet most users will undoubtedly at some point require the total OSCAR currents. In this section we describe direct comparisons between the total OSCAR currents and drifting buoy velocities over the period Oct. 1992-2003, and across the tropical Pacific as divided into nine roughly  $60^\circ$  longitude by  $20^\circ$  latitude sub-areas (Fig. 11).

As before drifter velocities and positions were 20-day low-pass filtered along the drifter trajectory and then paired with matching OSCAR velocities interpolated to the times and locations of the drifter data. For this analysis, however, we did not remove any mean velocity field from the data. Rather, in order to help evaluate the contributions of the mean and time-varying OSCAR signals we compare the total drifter velocities to three versions of the OSCAR data: (case 1) the total OSCAR field, (case 2) the OSCAR seasonal cycle, and (case 3) the OSCAR long-term mean. Both the long-term mean and the mean seasonal cycle are computed over the 1993-2003 period. Independent comparison statistics for zonal and meridional velocity are obtained for each of the three cases in each sub-area (Table 1). Correlation is defined as

usual, while skill is defined as  $sk = 1 - \text{rms}(\text{drifter-OSCAR})/\text{rms}(\text{drifter})$ : note that the OSCAR velocity's relative error is  $1-sk$ . In almost all sub-areas correlation and skill increase as one progresses from the time mean through seasonal to total OSCAR fields, indicating the positive contribution of the time-varying OSCAR signal in replicating drifter velocities. Nevertheless a substantial fraction of the skill is found in the mean field alone, especially for meridional velocity, as is to be expected in a region with strong mean currents.

Additional insight may be gained by examining individual monthly maps to determine how well specific circulation features are reproduced. Monthly maps are available on-line comparing drifter- and OSCAR-derived current vectors for the entire time period in each sub-area (by way of <http://www.oscar.noaa.gov/>), but here for brevity we present only a single map of the central equatorial Pacific (sub-area PAC2) during Dec. 2003 (Fig. 12). This monthly map contains 311 separate 5-day drifter vectors, and hence must include data from at least 51 drifters. As seen on the two maps on top of Figure 12, the OSCAR collocated vectors reproduce the drifter velocities well, and certainly provide a more comprehensive picture of the large-scale surface flow. The drifter data at this time cover several areas where flow pathways are apparent at the frontier between the South Equatorial Current (SEC) and the NECC. These pathways, located near 168°W, 160°W, 150°W, and 138°W, are notably well reproduced by the OSCAR vectors. Note the match is also good on the equator and to the south. Hence, the meridional structure of the OSCAR velocity in the equatorial vicinity is quite realistic. This indicates that the OSCAR methodology performs well at reproducing fine mean and time-varying structures of the flow field.

Figure 13 summarizes statistical results for all data in the PAC2 (central) region for the entire time period. The histograms of differences between drifter and co-located OSCAR

velocities are very close to Gaussian distributed, as shown by the superimposed Gaussian curves drawn with data-derived means and standard deviations. This allows the accumulated errors of calculations involving OSCAR currents to be estimated relatively simply.

## **5. Discussion**

### *a. Poleward deficit of variance*

A shortcoming common to all the surface current products studied here, both OSCAR- and GCM-derived, is an increasing deficit of product velocity variance relative to the drifters as one proceeds away from the equator (compare Figs. 6 and 7). Leeuwenburgh and Stammer (2002) found a similar result in their study involving GCM-derived SSHs sub-sampled along simulated satellite tracks: the fraction of current variability captured by the satellite relative to the true (original) variability decreased poleward from the equator. Similarly their RMS errors as a fraction of true variability increased moving poleward, comparable to our decreasing signal/noise ratios (Fig. 10). While no data presented here supports definitive conclusions, we speculate that the poleward decrease of space and time scales expected of a shrinking Rossby radius and inertial period contribute to increasingly severe aliasing of ocean variability by the relatively fixed spatial and temporal intervals of the satellite tracks (2.8 degrees longitude and ~10 days). Preliminary calculations of OSCAR currents at finer resolutions do in fact give higher amplitudes and slightly better correlations at higher latitudes. The use of multiple altimetric satellites when available should also improve fidelity (Leeuwenburgh and Stammer 2002) of a suitably resolved OSCAR product. While use of the AVISO multiple-satellite SSH product did not increase OSCAR's fidelity much here (Fig. 14), this is in part due to the canonical calculation subsampling SSH fields at one degree intervals. This provides adequate resolution for TOPEX/Poseidon data but under-samples higher-resolution products. Further

improvements of OSCAR currents, especially at higher latitudes, are a continuing research effort.

*b. Zonal/meridional asymmetry*

The steep angle of satellite tracks at low latitudes can produce larger meridional velocity errors than zonal velocity errors when the "cross-track" method is used: this is when cross-track geostrophic velocity is calculated directly from the SSH measured along the track and then resolved into geographic components where satellite tracks intersect. This disparity in errors is less of a problem when velocity is calculated directly from gridded SSH fields, probably because gradients between adjacent tracks help constrain the calculation. In such cases isotropic velocity fields have expected zonal and meridional errors differing only by a few tens of percent (Le Traon and Dibarboure 1999, Ducet et al. 2000, Schlax and Chelton 2003). We conclude the larger differences in the error found here are due to the markedly different statistics of zonal and meridional velocity in the tropical Pacific. Near-equatorial meridional velocity is dominated by tropical instability waves having wavelengths of ~1000 km and periods of ~15-20 days (e.g. Johnson and Proehl 2004). These scales are poorly resolved by Topex/Poseidon, and so result in poorly measured meridional velocities compared to the larger-scale, lower-frequency zonal currents. The fact that OSCAR meridional velocity accuracy improves by 8°N confirms that satellite track orientation is not the major problem.

*c. Comparison to ECCO models*

In general the OSCAR algorithm produces better surface current signal/noise ratios than the ECCO simulations despite the latter's assimilating all the constituent OSCAR data plus additional data, such as the time-mean of drifters used here for validation (ECCO1) or their

temporal variability (ECCO2). Several factors contribute to this. First, the ECCO1 model assimilates a climatological seasonal cycle along with time resolved data, thus biasing its results toward the seasonal cycle at the expense of other variability. This can produce substantial errors in our study region since the tropical Pacific has substantial variability at both shorter and longer time-scales. Secondly, when assimilating noisy data the least-square-error optimizations used in the ECCO models will bias the response amplitudes toward zero in order to minimize the amount of data noise transmitted to the solution. In contrast the OSCAR algorithm attempts to reproduce a physically based response: the geostrophic current resulting from a given SSH gradient and wind stress. This approach will pass more noise but also more signal, generally giving a better signal/noise ratio. When comparing errors alone, that is the RMS difference between drifters and surface current product, OSCAR and ECCO velocities give a more similar performance (Fig. 14). For zonal velocity ECCO still has slightly higher errors, especially in the range from 2-10°N, while for meridional velocity the errors are closely comparable, or even smaller for ECCO in the equatorial western Pacific.

Thus when evaluating different surface current products it is worth considering what measure of goodness is most appropriate for a given use. The OSCAR product is probably more suited than ECCO models to applications requiring physically realistic velocities, such as search and rescue operations or tracer dispersion: statistically the RMS errors of the two calculations will be similar, but the OSCAR product's probability distribution will be more centered on the drifting object's true position, and less biased toward remaining in the starting position.

## **6. Summary and Conclusions**

Comparison of the OSCAR satellite-derived sea surface currents with ground truth data from MCM, drifter, and shipboard ADCP instruments indicate that the present OSCAR product

provides accurate estimates of zonal and meridional time-mean circulation, and in the near-equatorial region reasonably accurate estimates of zonal current variability (correlation = 0.5 to 0.8) at periods as short as 40 days and at meridional wavelengths as short as  $8^\circ$  (Figs. 8,9). This is confirmed by individual monthly maps showing drifter trajectories conforming to the large-scale velocity structures observed by OSCAR. At latitudes higher than  $10^\circ$  the correlation remains respectable but OSCAR amplitudes diminish unrealistically: the reasons for this are not entirely clear but are the subject of ongoing research. Variability of meridional velocity is poorly reproduced in general, with amplitudes badly underestimated and correlations smaller than those for zonal velocity, especially on the equator. This is attributable to the shorter time and space scales of meridional velocity in this region. RMS errors between drifters and OSCAR velocities are very similar to those experienced by the ECCO data-assimilating models; but OSCAR generally estimates a larger ocean-correlated signal which substantially enhances its ratio of estimated signal over noise. Phase lags between MCM currents and the wind-driven portion of OSCAR indicate that further increases in fidelity may be obtained in the 20-90 day band by incorporating a time derivative in the diagnostic momentum balance. Slightly better results are also obtained by substituting AVISO SSH fields into the OSCAR algorithm, especially in the 20-40 day band and for meridional velocity, indicating that improved gridding schemes can enhance OSCAR's fidelity even with presently available data.

*Acknowledgments:* Support from NOAA grants DG133E-02-CN-0075 and NA16GP2023 is gratefully acknowledged. We thank Sharon Lukas and Peter Niiler of UCSD for help with the AOML drifter data, Ichiro Fukumori (JPL/NASA) and Detlef Stammer (University of Hamburg) for guidance concerning their ECCO models, Greg Jacobs and Kirk Whitmer of NRL, and Pierre Yves LeTraon of AVISO for providing SSH fields. We are also indebted to other investigators

for making their data available: equatorial current data were downloaded from the TOGA-TAO website, and ADCP data were provided by Eric Firing via download from the NODC Joint Archive for Shipboard ADCP.

## References

- Atlas, R., R. Hoffman, S. Bloom, J. Jusem, and J. Ardizzone, 1996: A multi-year global surface wind velocity data set using SSM/I wind observations. *Bull. Amer. Meteor. Soc.*, **77**, 869-882.
- Bonjean, Fabrice, and Gary S. E. Lagerloef, 2002: Diagnostic model and analysis of the surface currents in the tropical Pacific ocean. *J. Phys. Oceanogr.*, **32**, 2938-2954.
- Ducet, N., P. Y. Le Traon, and Gilles Reverdin, 2000: Global high-resolution mapping of ocean circulation from TOPEX/Poseidon and ERS-1 and -2. *J. Geophys. Res.*, **105 (C8)**, 19,477-19,498.
- Emery, W. J., and Richard E. Thomson, 1998: *Data analysis methods in physical oceanography*. Pergamon, 634pp.
- Firing, Eric, Susan Wijffels, and Peter Hacker, 1998: Equatorial subthermocline currents across the Pacific. *J. Geophys. Res.*, **103**, 21,413-21,423.
- Fukumori, Ichiro, 2002: A partitioned Kalman filter and smoother. *Mon. Wea. Rev.*, **130**, 1370-1383.
- Johnson, Eric S., and Patricia E. Plimpton, 1999: TOGA/TAO shipboard ADCP data report, 1991-1995. NOAA Data Rep., ERL PMEL-67, 23pp.
- Johnson, Eric S., and Jeffrey A. Proehl, 2004: Tropical instability wave variability in the Pacific and its relation to large-scale currents. *J. Phys. Oceanogr.*, **34**, 2121-2147.

Kashino, Y., H. Hase, Kentaro Ando, K. Yoneyama, Y. Takatsuki, Y. Kuroda, and K. Mizuno, 2001: TOCS Data Report 2: 1995-2000. Ocean Observations and Research Department, Japan Marine Science and Technology Center, 2-15 Natsushima, Yokosuka 237-0061, Japan, TOCS No.4. 327 pp.

Lagerloef, Gary S. E., Gary T. Mitchum, Roger Lukas, and Pearn P. Niiler, 1999: Tropical Pacific surface currents estimated from altimeter, wind and drifter data. *J. Geophys. Res.*, **104**, 23,313-23,326.

Leeuwenburgh, Olwijn, and Detlef Stammer, 2002: Uncertainties in altimetry-based velocity estimates. *J. Geophys. Res.*, **107(C10)**, 3175, doi:10.1029/2001JC000937.

Le Traon, P. Y., and G. Dibarboure, 1999: Mesoscale mapping capabilities of multiple-satellite altimeter missions. *J. Atmos. Ocean Tech.*, **16**, 1208-1223.

Murray, J. W., Eric S. Johnson, and Chris Garside, 1995: A U.S. JGOFS process study in the equatorial Pacific (EqPac): Introduction. *DeepSea Res. II*, **42**, 275-293.

Pazan, Stephen E., and Pearn P. Niiler, 2004: New global drifter data set available. *EOS* **85(2)**, p17.

Reynolds, Richard W., Nick A. Rayner, Thomas M. Smith, Diane C. Stokes, and Wanqiu Wang, 2002: An improved in situ and satellite SST analysis for climate. *J. Climate* **15**, 1609-1625.

Rio M.-H. and F. Hernandez, 2004: A mean dynamic topography computed over the world ocean from altimetry, in situ measurements, and a geoid model. *J. Geophys. Res.*, **109**, C12032,

doi:10.1029/2003JC002226.

Santiago-Mandujano, F., and Eric Firing, 1990: Mixed-layer shear generated by wind stress in the central equatorial Pacific. *J. Phys. Oceanogr.*, **20**, 1576-1582.

Schlax, Michael G., and Dudley B. Chelton, 2003: The accuracies of crossover and parallel-track estimates of geostrophic velocity from TOPEX/POSEIDON and Jason altimeter data. *J. Atmos. Oceanic Tech.*, **20**, 1196-1211.

Stammer, Detlef, Carl Wunsch, R. Giering, C. Eckert, P. Heimbach, J. Marotzke, A. Adcroft, C. N. Hill, and J. C. Marshall, 2002: The global ocean circulation during 1992-1997, estimated from ocean observations and a general circulation model. *J. Geophys. Res.*, **107(C9)**, 10.1029/2001JC000888.

	RMS OF DIFFERENCE (cm/s)						CORRELATION						SKILL					
	TOTAL		SEAS.		MEAN		TOTAL		SEAS.		MEAN		TOTAL		SEAS		MEAN	
	u	v	u	v	u	v	u	v	u	v	u	v	u	v	u	v	u	v
R1	<b>16</b>	<b>14</b>	21	14	25	14	<b>.88</b>	<b>.47</b>	.78	.32	.68	.25	<b>.52</b>	<b>.07</b>	.38	.03	.28	.01
R2	<b>14</b>	<b>13</b>	21	13	24	13	<b>.86</b>	<b>.45</b>	.67	.33	.52	.31	<b>.51</b>	<b>-.03</b>	.28	-.02	.17	-.01
R3	<b>23</b>	<b>15</b>	30	14	32	14	<b>.69</b>	<b>.36</b>	.34	.23	.12	.14	<b>.23</b>	<b>-.15</b>	.00	-.08	-.06	-.10
R4	<b>8.2</b>	<b>8.0</b>	10	9.2	11	9.3	<b>.71</b>	<b>.58</b>	.50	.36	.36	.31	<b>.33</b>	<b>.18</b>	.18	.06	.11	.05
R5	<b>10</b>	<b>9.2</b>	12	11	12	11	<b>.73</b>	<b>.53</b>	.58	.17	.54	.11	<b>.38</b>	<b>.15</b>	.27	.02	.25	.01
R6	<b>12</b>	<b>11</b>	15	13	15	13	<b>.74</b>	<b>.59</b>	.55	.20	.49	.14	<b>.37</b>	<b>.20</b>	.23	.03	.20	.02
R7	<b>7.0</b>	<b>6.5</b>	7.7	6.8	7.8	6.9	<b>.52</b>	<b>.36</b>	.37	.22	.35	.18	<b>.25</b>	<b>.04</b>	.18	.00	.17	-.01
R8	<b>8.8</b>	<b>8.2</b>	10	9.0	11	9.0	<b>.65</b>	<b>.41</b>	.42	.09	.31	.06	<b>.25</b>	<b>.13</b>	.12	.03	.08	.04
R9	<b>11</b>	<b>11</b>	13	13	14	13	<b>.69</b>	<b>.53</b>	.46	.23	.33	.20	<b>.36</b>	<b>.16</b>	.24	.03	.18	.03

Table 1: RMS difference, correlation and skill (see text for definition) between drifting buoy velocities and collocated OSCAR calculations, for zonal and meridional components separately, for each region in Fig.11. The period of calculation is Oct.1992 to June 2004. Three versions of OSCAR velocities are compared: TOTAL is the total OSCAR velocity, SEAS is the 1993-2003 average seasonal cycle, and MEAN is the 1993-2003 time mean. The drifter data are the same in each case.

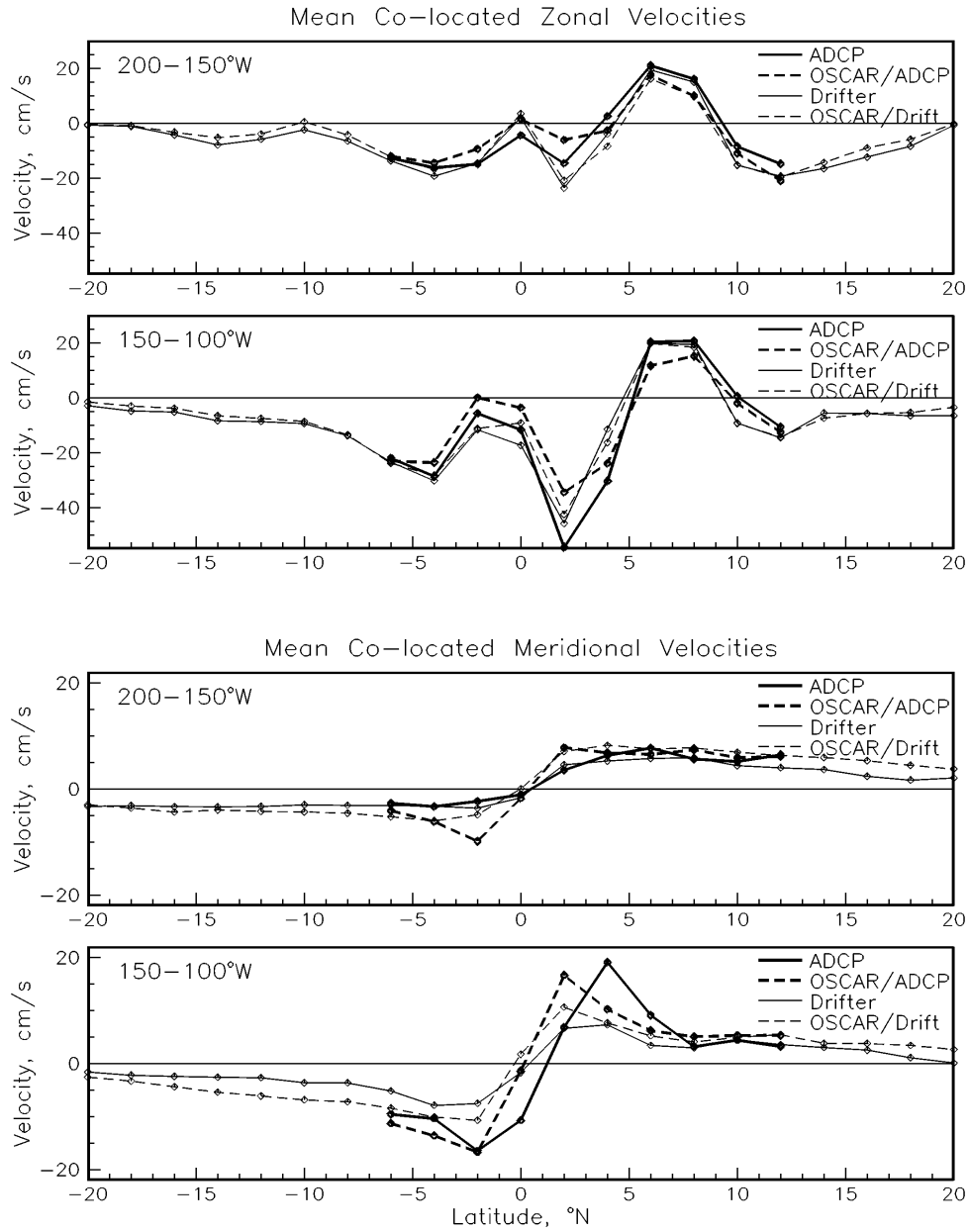


Figure 1. The time-averaged velocities from surface drifters (bold lines) and ADCP shipboard profilers (lighter lines), compared in each case to OSCAR currents (dashed lines) subsampled and interpolated to match the *in situ* data's times and positions. In each case data have been further averaged in 50° longitude by 2° latitude bins.

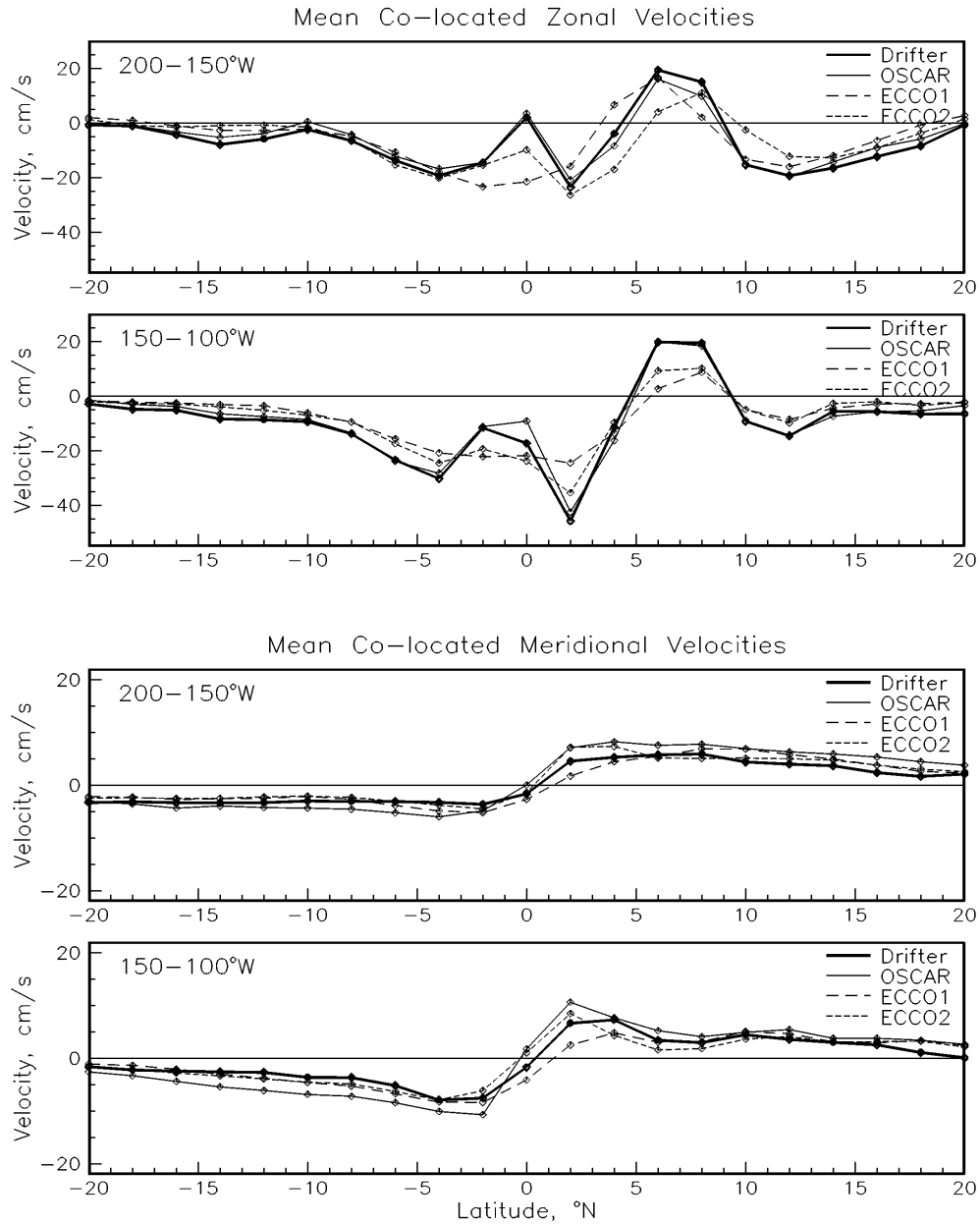


Figure 2. The drifter/OSCAR mean comparison from Figure 1 with additional means from the ECCO 1 and 2 models similarly sub-sampled to the drifter times and positions.

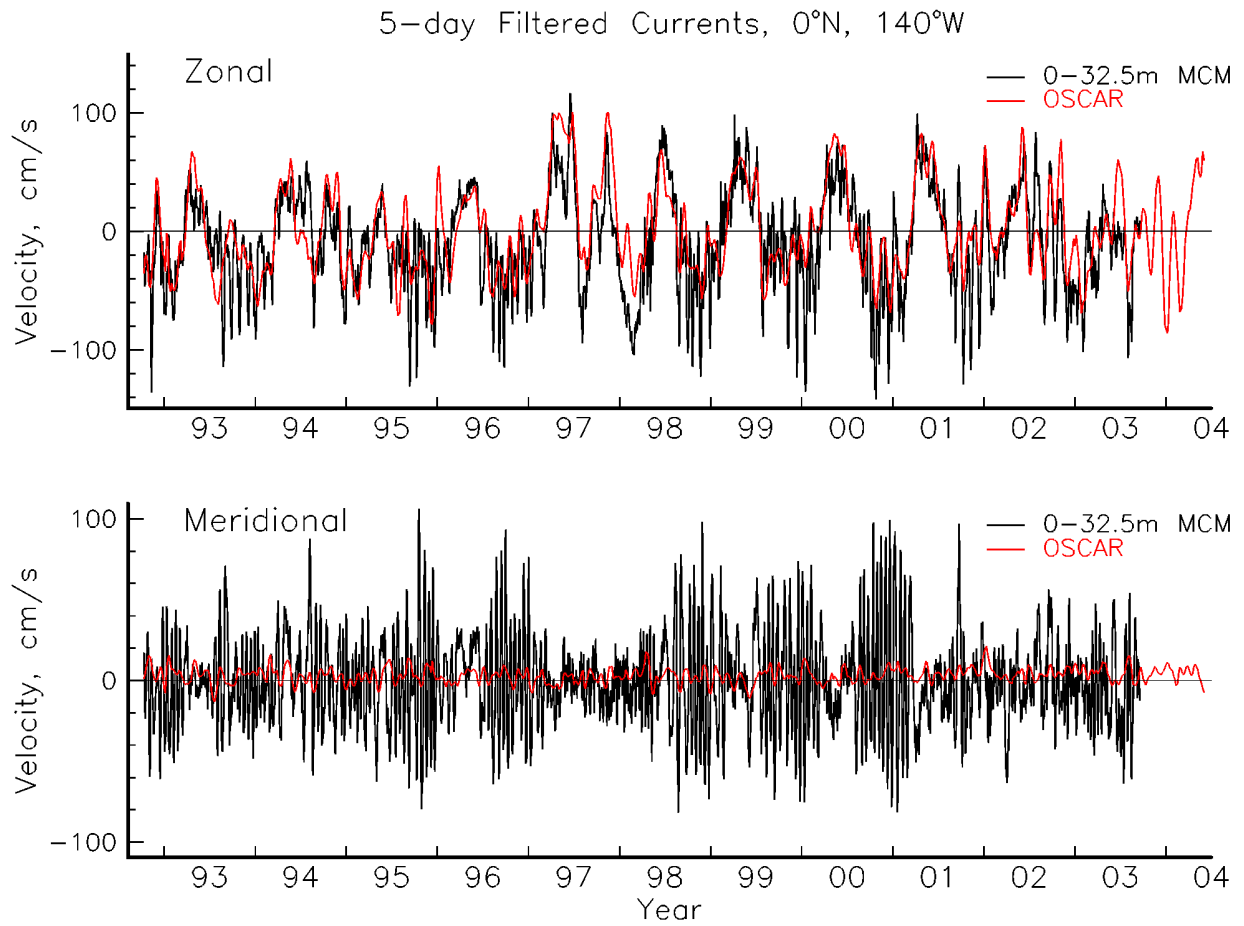


Figure 3. MCM currents at 0°N, 140°W averaged over the top 35.2 m and low-pass filtered to half-power at 5 day period, compared with OSCAR satellite-derived currents interpolated to the same times and positions.

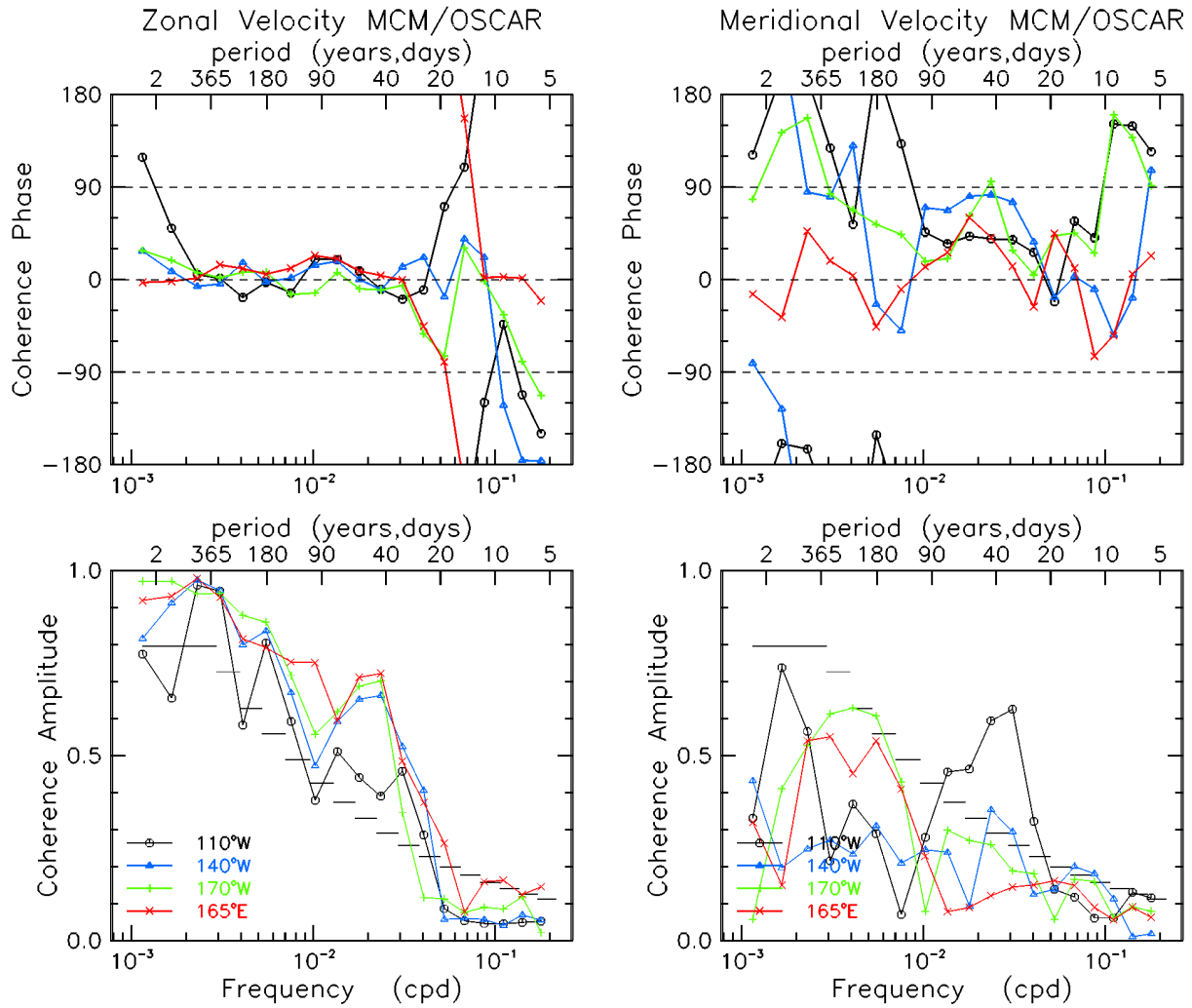


Figure 4. Coherence between OSCAR and equatorial MCM velocities at 4 longitudes. Positive phases imply MCM leads OSCAR. 95% significance levels for amplitude are shown.

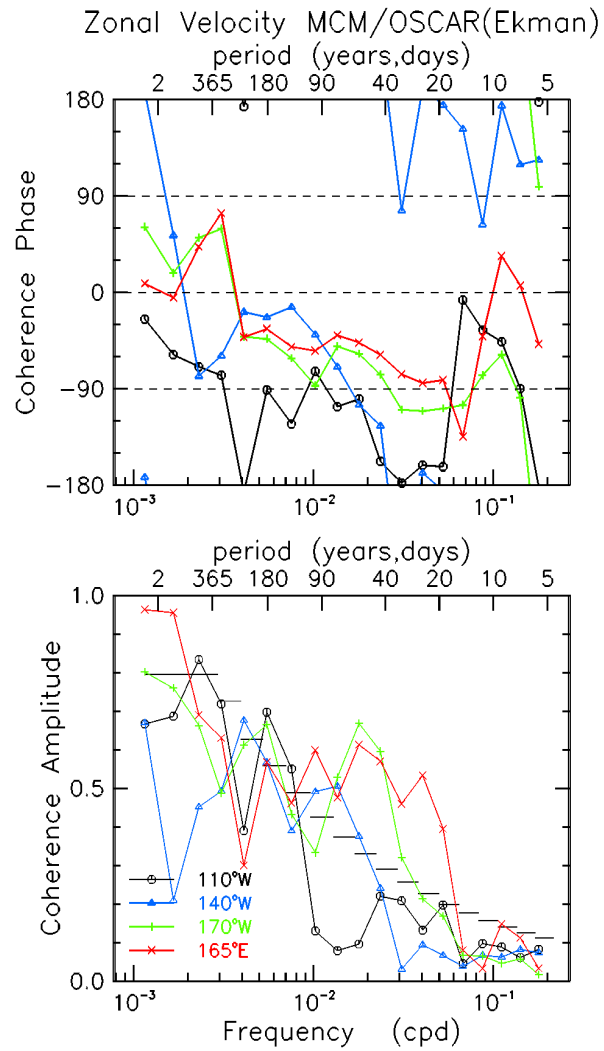


Figure 5. Coherence as in Fig. 4 but for the wind-driven, Ekman component of OSCAR zonal velocity without the pressure- and buoyancy-driven components.

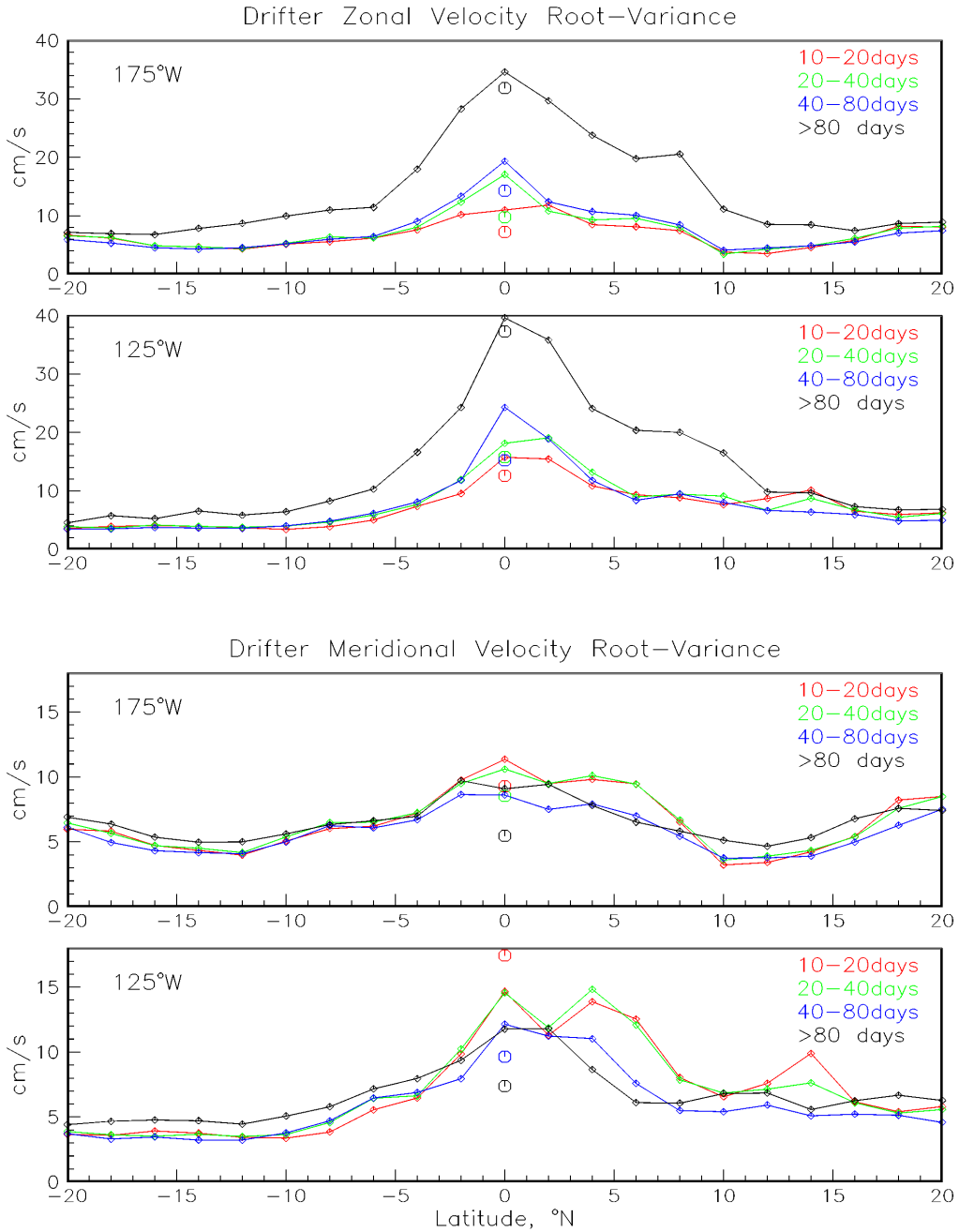


Figure 6. RMS variability of drifter velocities about the data mean of Fig. 1, binned in latitude and longitude as in that figure. The root-variance has been separated into period bands with the ranges shown using filtering techniques (see text). Comparable MCM root-variances at the equator are shown as small circles.

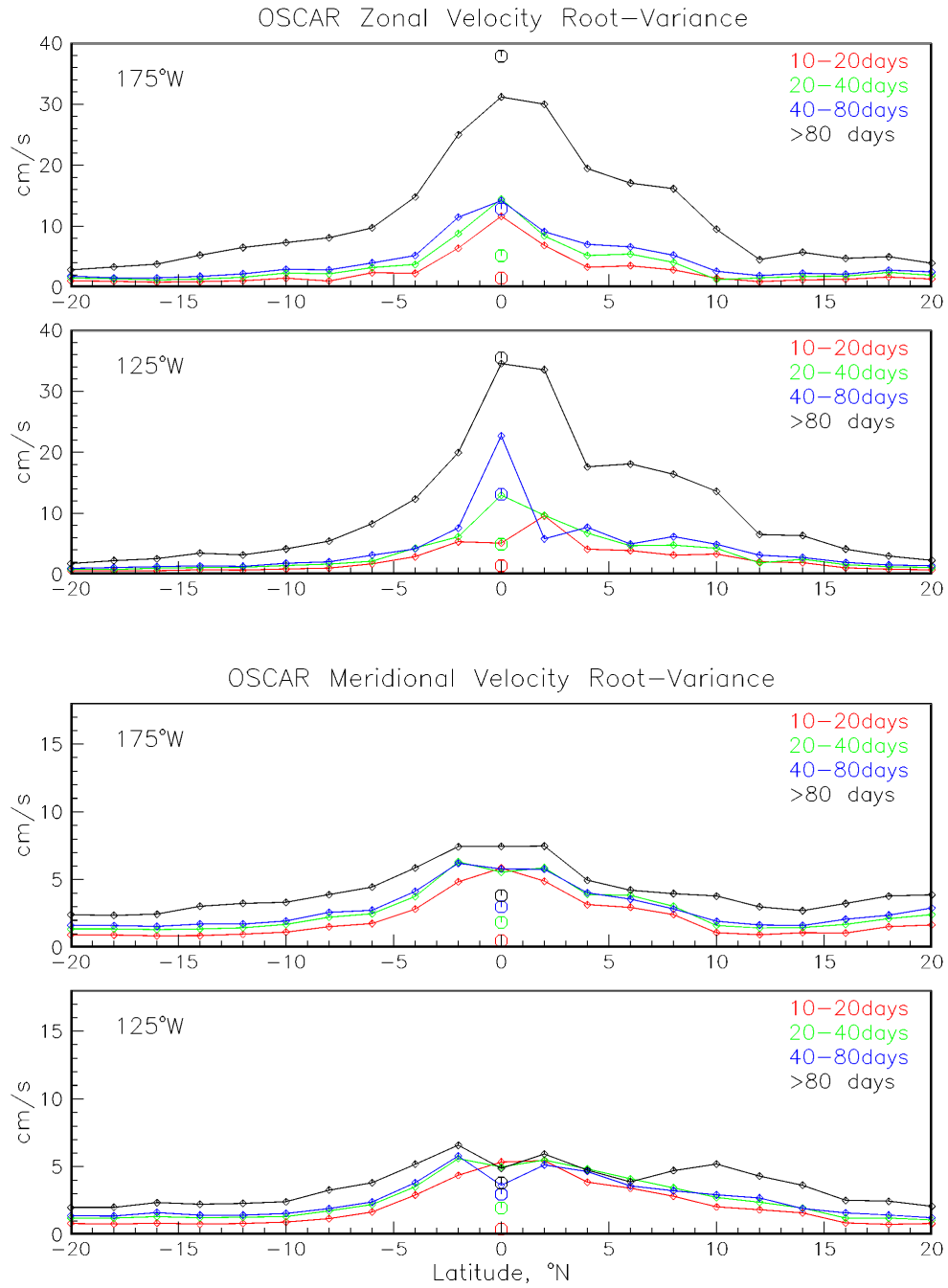


Figure 7. As in Fig. 6 but for OSCAR currents matched to the drifter tracks as in Fig. 1.

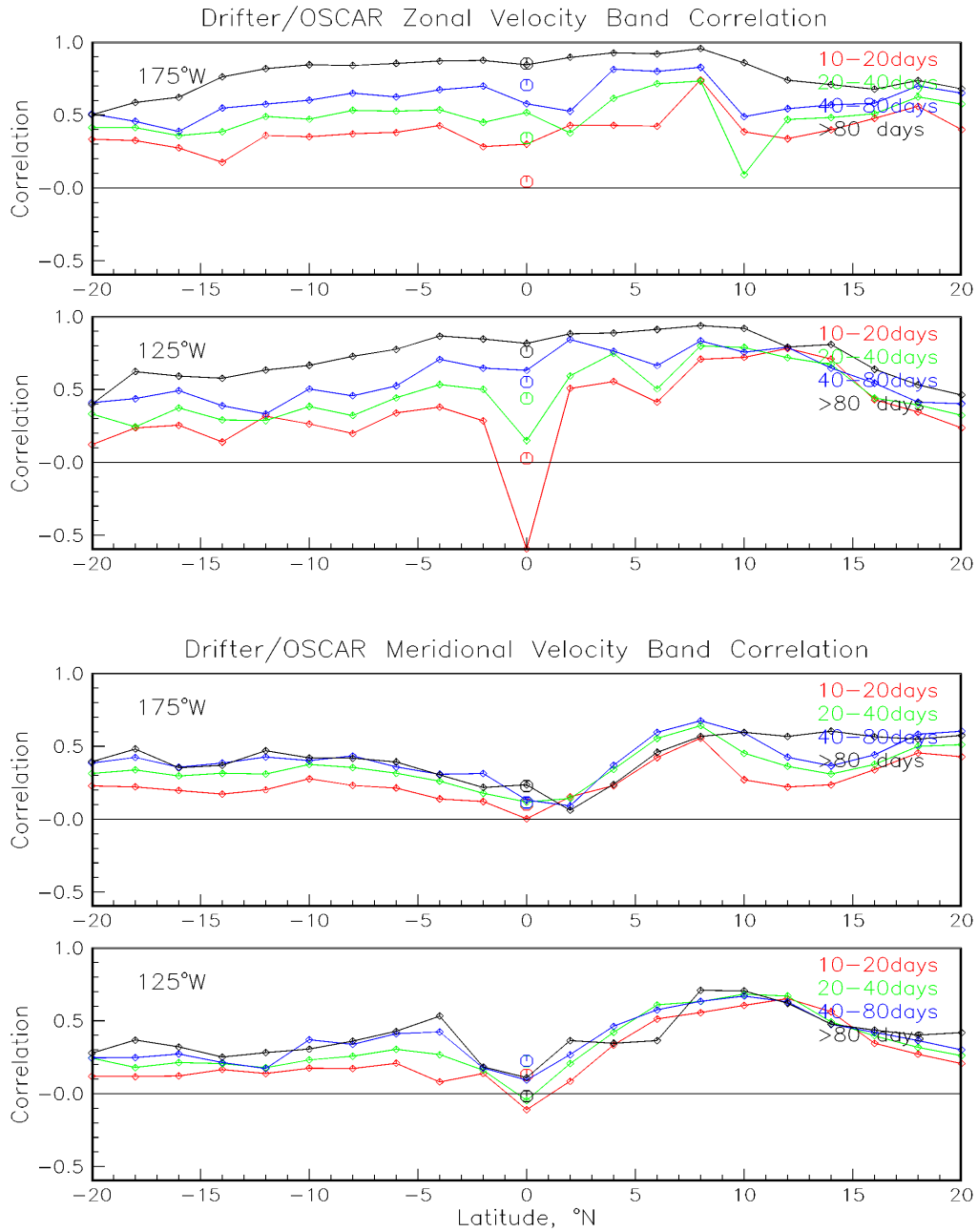


Figure 8. As in Figs. 6 and 7 but for correlation between drifter and matched OSCAR currents.

Wavelength Band-passed RMS Velocities and Correlation

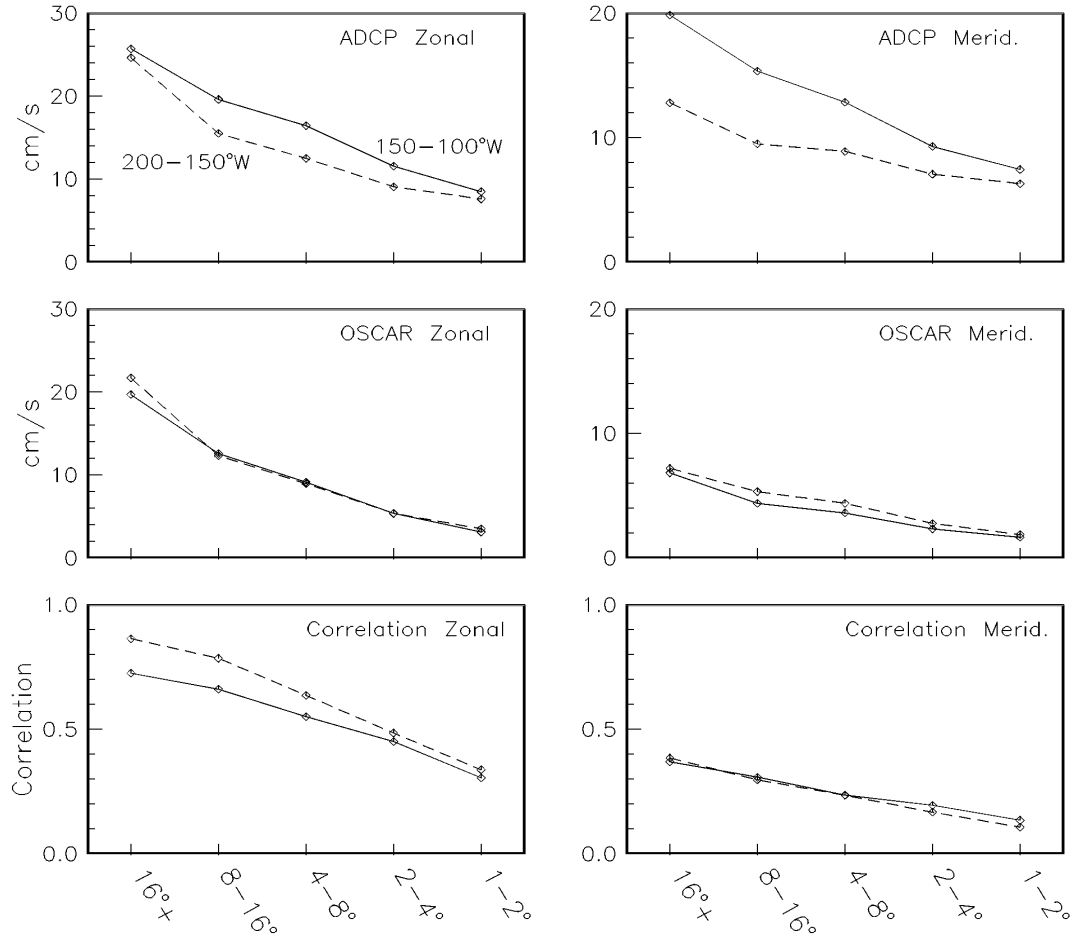


Figure 9. RMS velocity variability from meridional sections of shipboard ADCP data and matched OSCAR currents, filtered meridionally into wavelength bands in analogy to the time analysis of Figs. 6-8. Data were further averaged in 50° longitude bins as before. Top panels, ADCP variability; middle panels, matched OSCAR variability; bottom panels, their correlation.

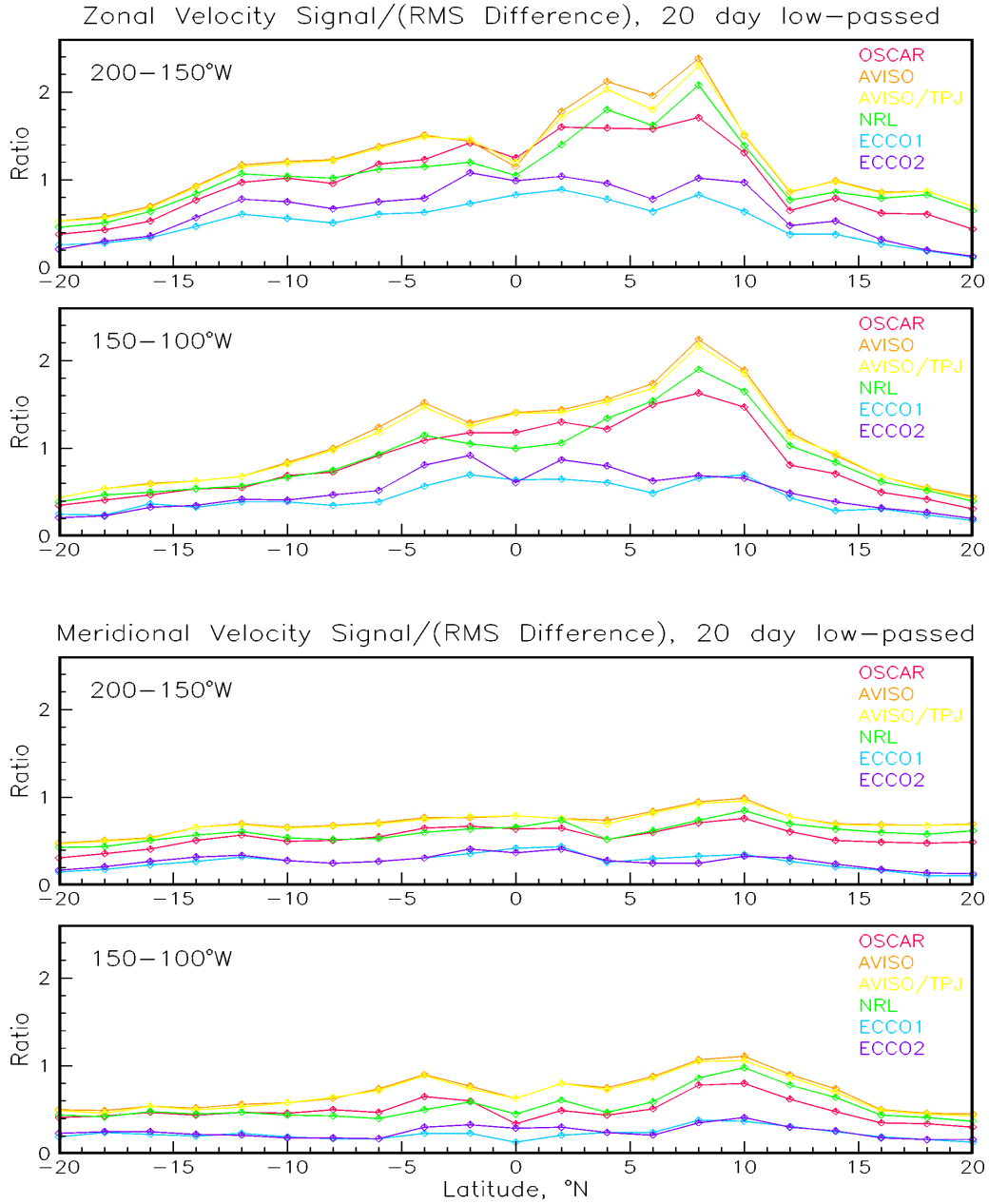


Figure 10. The ratio of calculated velocity over RMS difference from drifters for various surface current products interpolated to the drifter times and locations as before. The OSCAR, AVISO, and NRL curves represent the OSCAR algorithm using various SSH products, while the ECCO curves are two versions of a data-assimilating ocean GCM (see text).

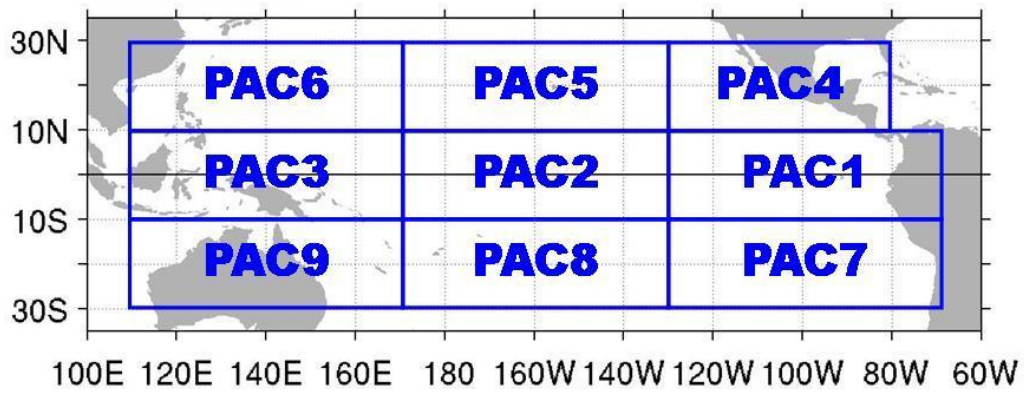


Figure 11. The nine sub-regions of the tropical Pacific Ocean in which the OSCAR currents are compared to WOCE drifting buoy data.

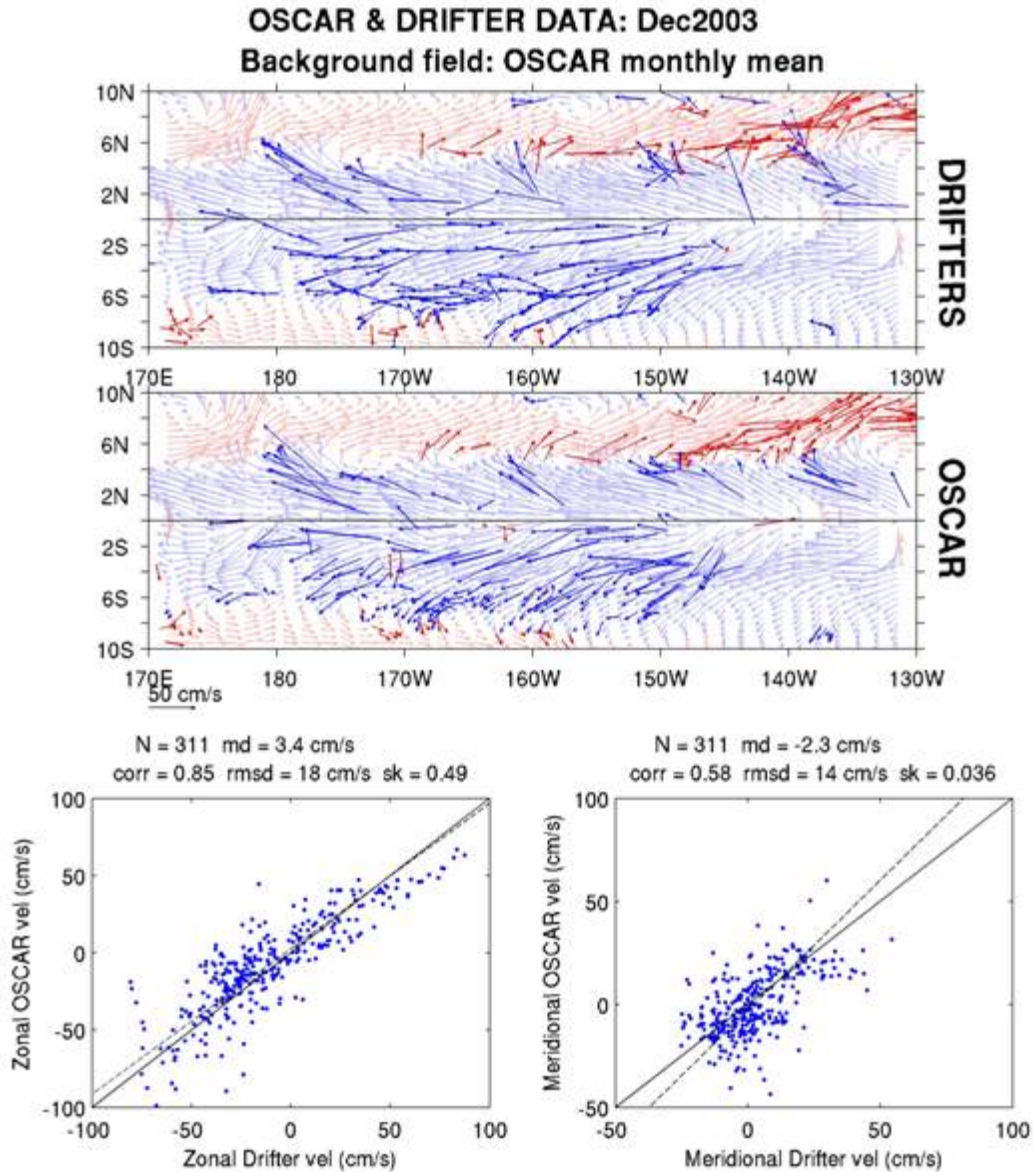


Figure 12. (Top two panels) Comparisons between drifting buoy and OSCAR velocity vectors during December 2003 in the central equatorial Pacific Ocean (PAC2). Background, faded vectors in both panels are the month-averaged OSCAR velocity field (red for eastward, blue for westward); superimposed dark vectors are (top map) 5-day averaged drifter velocities and (second map) co-located OSCAR velocities. (Bottom panels) Scatter plots of drifter versus co-located OSCAR velocities. Solid line is  $y=x$ , dashed line is the neutral regression line (e.g. Emery and Thompson 1998, p.247) between the two data sets. N is the number of data in this month and region, md the mean difference, corr the correlation and sk the skill (defined in text).

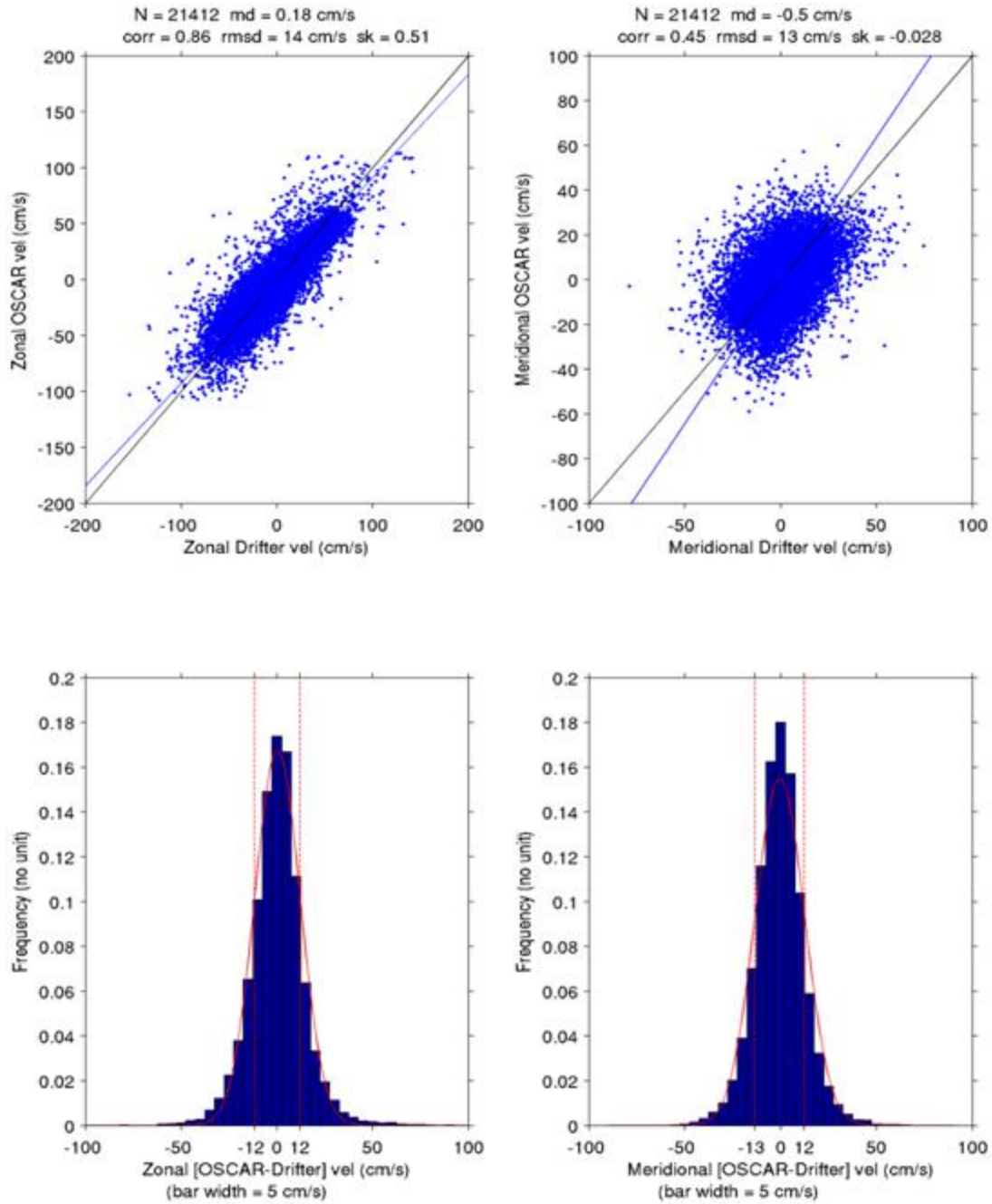


Figure 13. (Top) Scatter plots of the drifter versus the OSCAR velocity for the PAC2 region as in Fig. 12 but over the entire period Oct. 1992-June 2004. (Bottom) Histograms of the difference between the OSCAR and drifter data for the PAC2 region over the entire period. The red curves are Gaussian functions plotted using the data means and standard deviations, with vertical dashed lines marking one standard deviation from the means.

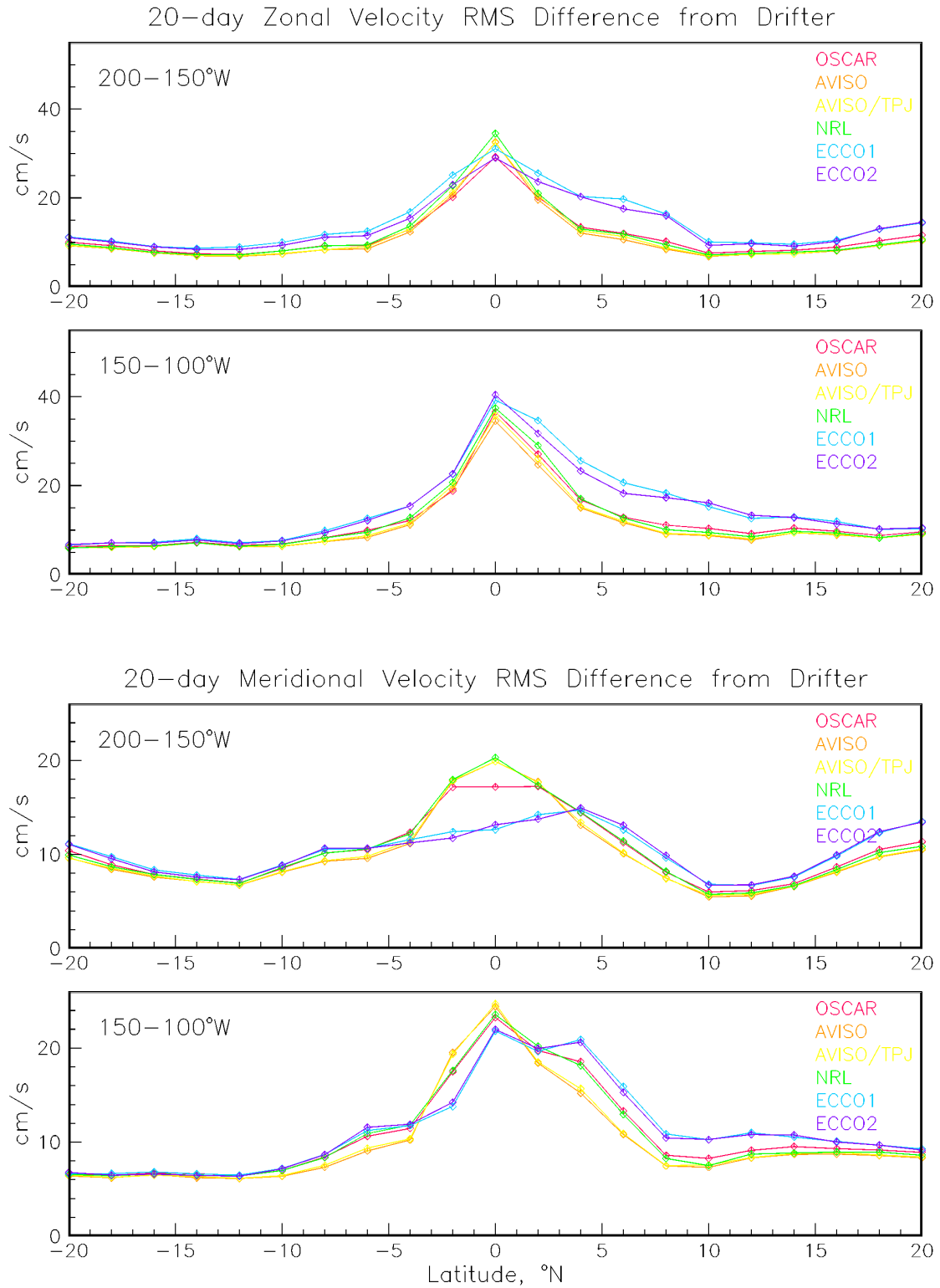


Figure 14. As in Fig. 10 but for the RMS difference between drifters for various surface current products.